Anisotropy of ultrasonic propagation and scattering properties in fresh rat skeletal muscle *in vitro*

Karen A. Topp and William D. O'Brien, Jr.
Bioacoustics Research Laboratory, Department of Electrical and Computer Engineering, University of Illinois at Urbana-Champaign, 405 North Mathews Avenue, Urbana, Illinois 61801

(Received 13 February 1999; revised 1 May 1999; accepted 6 October 1999)

The anisotropy of frequency-dependent backscatter coefficient, attenuation, and speed of sound is assessed in fresh rat skeletal muscle within 5 h *post-mortem*. Excised rat semimembranosus and soleus muscles are measured in 37 °C Tyrode solution, with the muscle fibers at 90° and 45° orientations to the incident sound beam. Reflected and through transmission signals from either a 6- or 10-MHz focused transducer give frequency dependent information in the 4–14 MHz range. The attenuation coefficient in each muscle is consistently a factor of 2.0 ± 0.4 lower for propagation perpendicular to the fibers than at 45°, whereas speed of sound shows a much milder anisotropy, and is slightly faster for the 90° orientation. The largest anisotropy is seen in the backscatter coefficient, most notably in the semimembranosus where the magnitude at 90° is over an order of magnitude greater than at 45°, with the frequency dependence in both cases giving a power law between 1.5 and 2.0. © *2000 Acoustical Society of America.* [S0001-4966(00)05401-1]

PACS numbers: 43.80.Cs, 43.80.Ev [FD]

INTRODUCTION

The variation of acoustic properties with direction of the incident sound field relative to the orientation of the medium being studied is known as acoustic *anisotropy*. Anisotropy in ultrasonic parameters characterizing biological tissue has been reported for a number of tissues with oriented structures, primarily myocardium,[1–8] in which Miller *et al.* have shown that attenuation is over a factor of 2 greater along the muscle fibers than perpendicular to them,[3] that speed of sound also has a maximum along the muscle fibers,[4] and that backscatter exhibits a maximum for incident sound perpendicular to the fibers and a minimum for for parallel incidence.[1,8] Tendon[5–7,9] and kidney[10] have also been studied for their anisotropic properties. The use of skeletal muscle to investigate ultrasound parameter anisotropy has primarily looked at bovine muscle; mostly attenuation[9,11–13] with an additional study each of speed[9] and integrated backscatter coefficient.[11] Investigations using dog,[14] rabbit,[14,15] and frog[15] muscles have measured speed of sound alone.

The great majority of the work cited above has been performed on samples which were fixed, frozen, or *post-rigor*, and the few studies using fresh tissue have measured only a single parameter at a time.[2,13,15] The aim of this study is to characterize the anisotropy of the frequency-dependent backscatter coefficient $\sigma_b(f)$, attenuation $\alpha(f)$, and speed of sound c, all measured at effectively the same time, in freshly excised rat skeletal muscle. Samples are measured in 37 °C Tyrode solution[16] to prolong the viability of the tissue and to create conditions as similar as possible to *in vivo*, which should be more clinically relevant than previous non-fresh anisotropy studies. Results are presented for ten rat soleus muscles, and ten rat semimembranosus muscles, both muscle types characterized by having straight and parallel muscle fibers.

I. METHODS

A. Muscle specimen preparation

The two muscle types studied here are both parallel-fiber skeletal muscles found in the leg of the rat; the soleus in the lower leg (the calf) and the semimembranosus in the upper lateral thigh. Adult rats (Sprague Dawley, Harlan, Indianapolis) were used for this study on fresh muscle, rather than using larger animals, since surplus rats from other investigations were readily available. Each muscle was excised from the rat within 15 min of when it was euthanized by CO_2. The experimental protocol was approved by the campus' Laboratory Animal Care Advisory Committee and satisfied all campus and NIH rules for the humane use of laboratory animals.

The excised semi-membranosus muscles were roughly rectangular in shape with typical relaxed dimensions of 2.0–2.5 cm long, 1.2–1.5 cm wide, and 0.5–0.7 cm thick; the sample is interrogated through its ''thickness'' which is remarkably flat and parallel over the region investigated, as determined from the acoustically detected front and back surfaces (see below). The soleus muscle samples were typically 2.0 ± 0.4 cm long between the tendons at each end. The fibers run neatly between tendons, lying straight and nearly parallel as the muscle is slightly thicker in the middle and tapers gradually to the ends. The muscle is interrogated through the thickest section, typically 0.3–0.4 cm thick (and 0.4–0.6 cm wide).

The microstructure of the two muscle types is shown in the stained microscope images of Fig. 1, in which the muscle fibers are seen in cross-section. The predominant feature in both images is the closely packed arrangement of muscle fibers, each surrounded by its sheath of connective tissue.

Within 5 min of excision, the muscles were fastened to a measurement holder such that the fibers were at a ~10%–20% stretch from relaxation. Soleus muscles were tied with suture through the tendons at each end, and the larger semi-

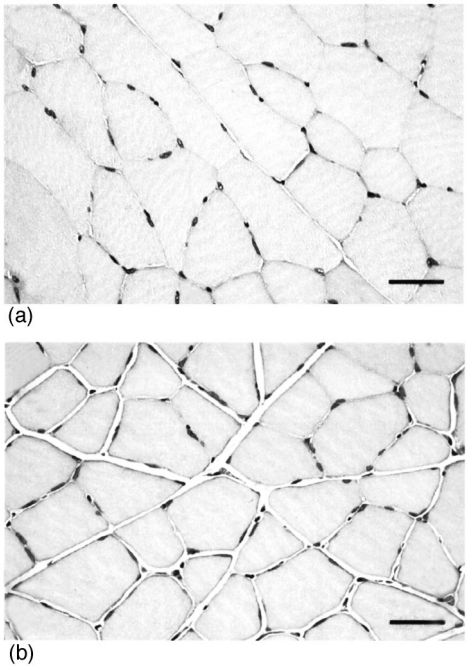

FIG. 1. Photomicrographs of the two rat muscle types, with the semimembranosus in the top panel (a) and the soleus below (b). The length scale in each image is determined by the bar which represents 50 μm. Muscle specimens were fixed in 10% neutral-buffered formalin, sectioned perpendicular to the fiber direction to 3 μm, and stained with hematoxylin and eosin for evaluation.

membranosus samples were held in place by a small stainless steel clip at each end. The sample was immediately immersed in a 37 °C Tyrode solution[16] (which was prepared with distilled degased water to limit gas formation) where it remained for all measurements. Tyrode solution is a nutritive medium containing the salts and glucose necessary to preserve cellular function in the tissue and thus maintain the viability of the sample for several hours. By removing a second (soleus) muscle from an animal, and holding it in similar conditions during the course of the experiment, we ascertained that the measured sample does not go into rigor for at least 4–5 h after death, by which time the acoustic measurements are completed.

B. Acquisition of data

The muscle sample, transducer, and needle hydrophone were all immersed in a temperature controlled ($37\pm0.5\,^{\circ}$C) Tyrode bath in an arrangement that allowed both transmission through, and reflection from, the same spatial locations in the muscle (see Fig. 2). The sample was held at the focus of either a 6-MHz or 10-MHz (Panametrics V309, V311) spherically focused transducer (both 1.27 cm diameter, 5 cm radius of curvature) which was excited by a Panametrics 5900 pulser/receiver. The reflected signal, and the through transmission signal from the 0.6-mm diameter needle hydrophone (Medicoteknisk Institut 1094) just behind the sample, were both received and amplified by the pulser/receiver and displayed on a LeCroy 9354 TM digitizing oscilloscope, set at 250 Ms/s. A dedicated PC recorded and stored the rf-signals from the oscilloscope for processing off-line.

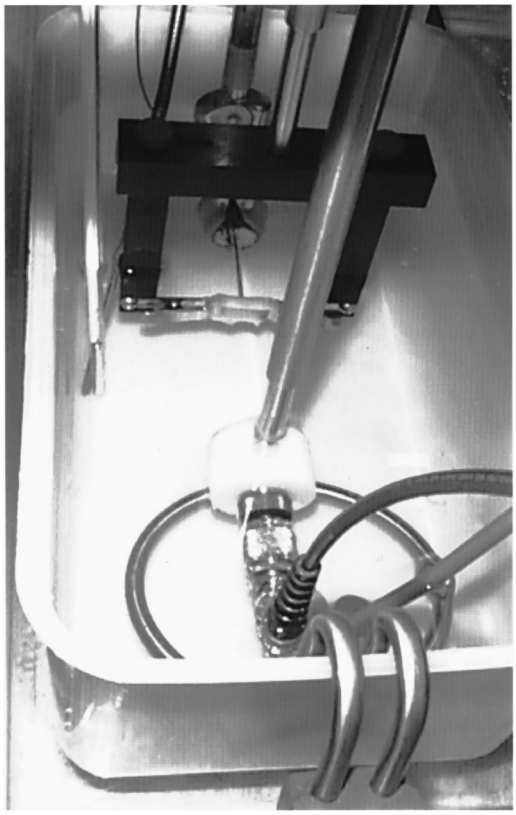

FIG. 2. Photograph showing the experimental apparatus. To determine the scale, note the semimembranosus muscle shown here is fastened in a holder whose black top bar measures 11 cm long. The needle hydrophone is directly behind the muscle, and the transducer is in the foreground. A heating coil and mechanical stirrer are seen below the transducer, and the heater's thermostat and a thermometer are seen to the left of the sample. All components are immersed in 37 °C Tyrode solution.

The muscle holder is moved within the sound field by a micropositioning system, which allows translational and rotational movement with a positional accuracy of 2 μm and 0.02 degrees, respectively. Two orientations with respect to the muscle fibers were measured: 90° (perpendicular) and 45°. (The effect of oblique incidence of the sound beam on the muscle surface in Tyrode was calculated for the 45° case to give a pressure transmission coefficient of greater than 0.998, in comparison to the normal incidence value of 0.999.) At each orientation, a 5×5 grid of spatial samples each separated by 700 μm (greater than both transducers' -6-dB spot size) was measured, with the muscle moved axially as necessary to ensure that the focal point of the transducer was at its center. Two rf-waveforms were captured for each spatial point: (a) a backscattered temporally averaged waveform (of 500 echoes) encompassing the entire muscle depth and both surfaces (to be gated off-line), which is used to find $\sigma_b(f)$ as well as the thickness of the sample at that spot; and (b) a transmission signal through the muscle. Between each spatial point measurement, the muscle is positioned out of the beam path to record (c) a reference transmission signal through the Tyrode solution alone. The two transmission rf-signals, (b) and (c), each averaged 100 times, are used to find $\alpha(f)$ and c. At the end of the experiment, a reference reflection signal for the σ_b measurement is collected from a flat Plexiglas plate positioned where the axial

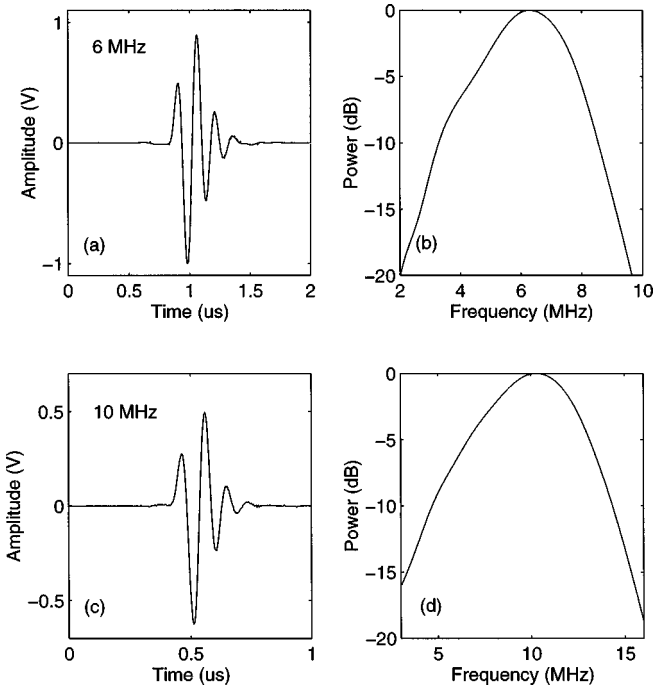

FIG. 3. Waveforms and power spectra of the two transducers used in this study; (a) and (b) from the 6-MHz transducer; (c) and (d) from the 10-MHz transducer. The waveforms are temporal averages of 100 echoes and were sampled at 250 MS/s.

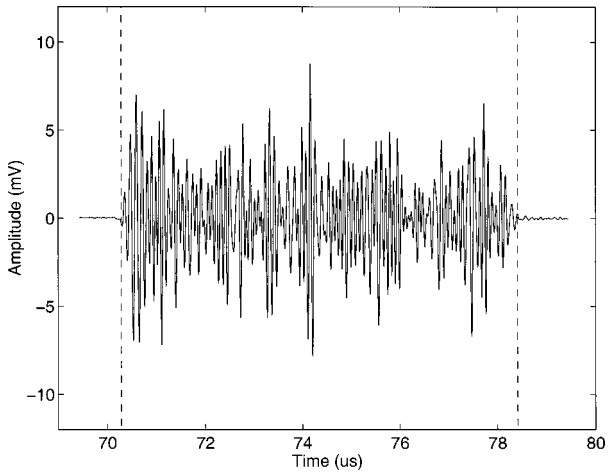

FIG. 4. The backscattered signal from a rat semi-membranosus muscle at 90° orientation to the sound beam. Dashed vertical lines are determined from an algorithm to find muscle surfaces $t_{1,2}$.

center of the muscle had been. Figure 3 shows the waveforms and corresponding spectra of the echo of each of the transducers from the Plexiglas plane reflector.

The freshness of the muscle samples was fundamental to the protocol of this study. Since the acquisition of data for each muscle took approximately 3 h (due to the spatial sampling and extensive signal averaging after nearly 1 h of positioning and setup time), each muscle was interrogated with only one of the two transducers to ensure that all measurements were completed within 4–5 h before the onset of rigor.

To ensure that the differences we may see at the two orientations were not a function of the aging of the muscle, six of the ten rat muscles of each type were measured at 90° orientation first before being turned to 45°, and four in reverse order. No difference was seen between these two populations in any of the measured acoustic parameters.

The effect of refraction of the sound beam through the muscle samples held at 45° has been carefully considered: A calculation of the beam through the thickest specimens of 7 mm (and most samples were thinner), using speeds of sound 1590 m/s and 1537 m/s for the muscle and Tyrode solution, respectively, gives a 0.36-mm lateral shift of the beam relative to the incident beam axis. This is about half the size of the hydrophone diameter, and about one-quarter of the −3-dB transducer beamwidth at the hydrophone. Since the hydrophone is mounted on micrometer positioners, a ''reoptimization'' of its position was attempted after turning the sample from 90° to 45°, but no increase in the through transmission signal magnitude was seen, and it was decided that less error was introduced into the measurement by simply leaving the relative positions of the transducer and hydrophone fixed. To check the refraction effect on a known isotropic, homogeneous substance, the attenuation at 45° and 90° through a 0.5-cm wide disk of Dow Corning silicone fluid (with Reynolds plastic wrap windows) was measured in water with the same equipment and without repositioning the hydrophone. The larger discrepancy in speeds of sound between water and silicone fluid (1486 m/s and 1390 m/s, respectively, at room temperature) made the calculated lateral beam shift 0.43 mm when the 0.5-cm disk was held at 45° to the incident beam axis. The measured attenuation of the silicone oil for the two orientations was less than 5% different over the whole frequency range of the 5-MHz transducer; thus we concluded that for the muscle samples, with more similar speeds of sound to the surrounding fluid bath, the refraction effect would cause only a few percent decrease at most in the received signal power at 45°, and could be ignored.

C. Analysis of data

Attenuation measurements require knowledge of the sample thickness, but since it is difficult to physically measure fresh tissue thickness, we use a technique employing the pulse times-of-flight (TOF) to the hydrophone with and without the specimen in the beam path (T_m and T_w, respectively), and the TOF back to the transducer from both muscle surfaces (t_1 front, t_2 back). See Fig. 4 for an example of the backscattered signal with the $t_{1,2}$ surfaces determined by an algorithm which looks for the first and last points which are greater than three times the baseline amplitude. (This baseline is defined as the average of the absolute value of the first 100 points—0.4 μs—of the captured waveform, which are arranged to be before the front surface of the sample.) Note the time difference between front and back surfaces is corrected in the analysis for the transmitted pulse duration, Δ (0.42 μs and 0.23 μs for the 6- and 10-MHz transducers, respectively). We calculate the speed of sound in the muscle, c_m, by:[17]

$$c_m = c_w\left[1+\frac{2(T_w-T_m)}{t_2-t_1-\Delta}\right], \tag{1}$$

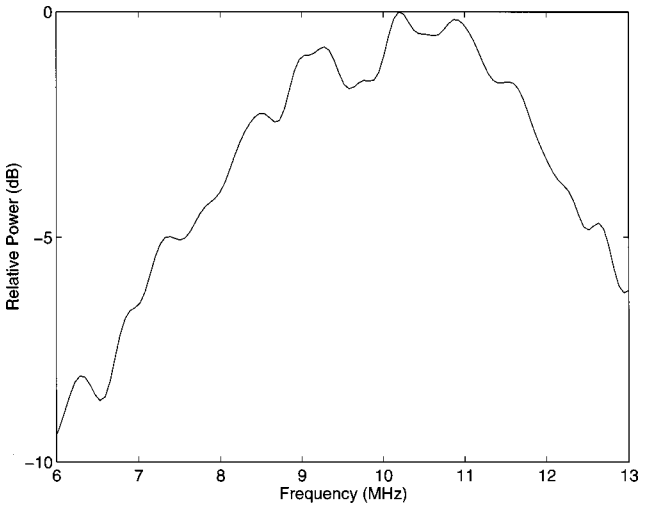

FIG. 5. Example of the echo spectrum from a semimembranosus muscle sample, measured with the 10-MHz transducer.

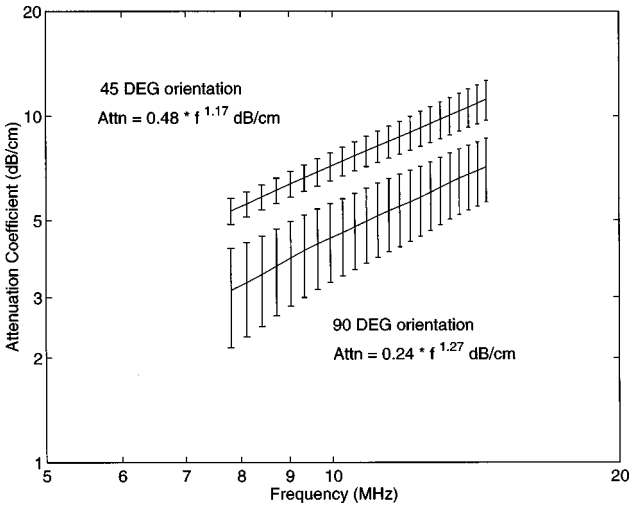

FIG. 6. Example of attenuation coefficient in a single muscle (semimembranosus #1) at 45° and 90°. Data are shown over the −5-dB bandwidth of the received hydrophone signal for the 10-MHz transducer, although the fit (not shown) is performed over −3 dB. Expressions for the best fit to each orientation are given in the figure, where f is in MHz. Error bars are the standard deviation of the 25 spatial samples in each case.

where c_w is the measured speed of sound in the Tyrode solution (1538 m/s at 37 °C). Then $c_m(t_2-t_1-\Delta)/2$ is the thickness of the muscle at that point. With thicknesses known, attenuation is then calculated by the insertion loss technique, in which the power spectrum of the signal transmitted through the sample is simply compared to the power spectrum received without the sample in the sound path.

Absolute backscatter coefficient is determined according to the method of Insana and Hall[18,19]

$$\sigma_b(f)=\frac{0.36R_1^2\gamma^2}{A_0\Delta z}e^{+4(\alpha_m-\alpha_0)(R_s+\Delta z/2)}\frac{\langle|S(f)|^2\rangle}{|R(f)|^2}, \qquad (2)$$

where R_1 is the average distance between the transducer and the near surface of the sampled volume, A_0 is the area of the transducer aperture, Δz is the axial length of the sampled volume, R_s is the distance from the muscle front face to the near surface of the sampled volume, α_m and α_0 are the frequency-dependent attenuation coefficients of the sample (measured for each case) and Tyrode solution (assumed similar to water), respectively, and $\langle|S(f)|^2\rangle$ is the spatially averaged power spectral estimate from the laterally sampled, diffraction corrected, Hanning gated[20] backscattered waveforms. [See Fig. 5 for an example of $\langle|S(f)|^2\rangle$ from a semimembranosus muscle.] $|R(f)|^2$ is the reference power spectral estimate obtained from the reflection against the Plexiglas plane reflector—with amplitude reflection coefficient $\gamma=0.35$—evaluated at axial distance $R_1+\Delta z/2$. Note that a factor of 4 error in our previous backscatter analysis[21] has been found and corrected.

The gated window depth for backscatter analysis of the semimembranosus muscles was 5 μs (4 mm), starting 1 μs below the front surface (to avoid surface reflections), and for the thinner soleus muscles was necessarily smaller, 3 μs (2.4 mm) at 0.5 μs below the front surface, to ensure the same sampling volume on all samples of the same muscle type. To check the effect of window gate length, the semimembranosus data were also analyzed with a 3-μs window, starting also at 1 μs below the front surface. This analysis showed no significant difference to that with the 5-μs gate, as determined by the best fits to both analyses of the same data having the same amplitude and power law exponent within a few percent.

II. RESULTS

The attenuation coefficient in each muscle shows a distinct difference between measurement with the muscle fibers at 90° and 45° to the incident sound beam. An example of $\alpha(f)$ for a single muscle (semimembranosus #1) is shown in Fig. 6 where the lines are the spatial averages over a given muscle orientation and the error bars the standard deviation of the 25 spatial samples. In 17 of the 20 muscle samples measured, the error bars of the two orientations were well separated like this; in the other three, there was some over-

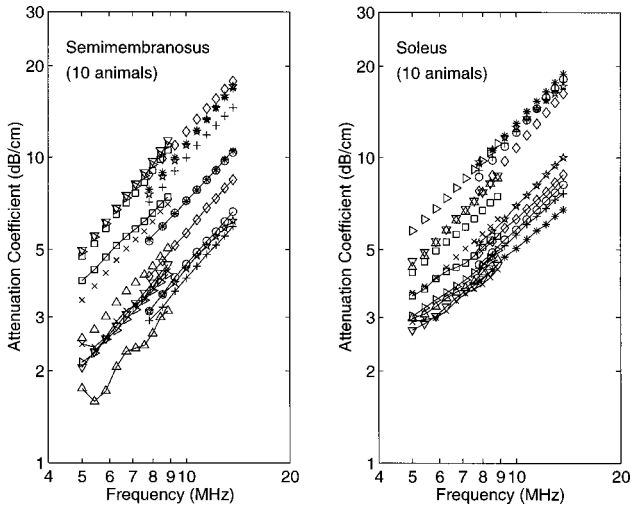

FIG. 7. Attenuation coefficient at 45° and 90° for the ten rat semimembranosus and ten rat soleus muscles. Different symbols represent individual muscles, where the higher valued data of each pair are the 45° orientation. For ease of distinction, the 90° orientation data have been connected with lines.

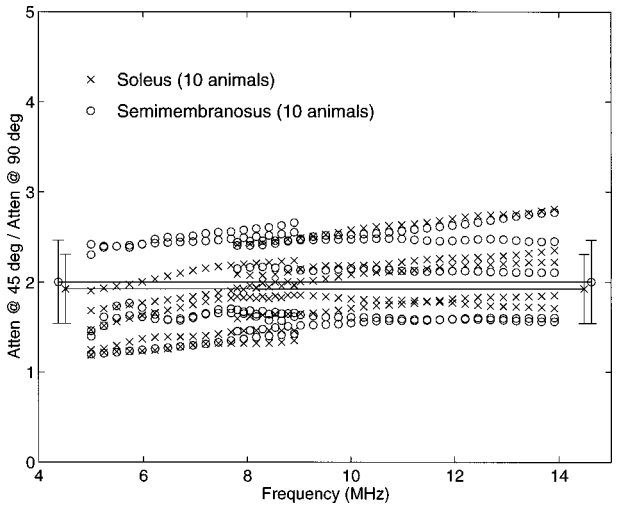

FIG. 8. Ratio of $\alpha(f)$ at 45° vs 90° for all 20 muscle samples. Solid lines represent the frequency-independent average of the $\alpha(f)_{45°}/\alpha(f)_{90°}$ ratio over the measured frequency range, and the error bars the standard deviation, for each muscle type ($N=10$).

lap. The average $\alpha(f)$ values for all 20 samples are shown in Fig. 7, where different symbols in each graph represent individual animals. Again, due to the time sensitivity of our measurements, a single muscle could not be measured with sufficient thoroughness at both orientations by both transducers, and so measurements on each sample are limited to the useful bandwidth of one transducer. For the purpose of distinction, the 90° orientation data are represented with both symbols and solid lines. The 45° data are always higher than 90°. Although the two orientations among all samples are not entirely separate, the ratio within each muscle stays fairly consistent (see Fig. 8). For both muscle types, the value of $\alpha(f)_{45°}/\alpha(f)_{90°}$ is very near to 2 (± 0.4) over the measured frequency range.

The averaged speed of sound values are given in Table I and plotted in Fig. 9. The difference between the two orientations in fresh muscle is only on the order of 0.5%, and the error bars here, due to the method of measuring thickness at each sampled location, have values close to the difference between orientations. Paired t-test analysis of the two orientations for each muscle type give probabilities of 0.006 and 0.0008 for the semimembranosus and soleus, respectively, that the speeds of sound for each orientation are from the same population. The observation that c at 90° is larger than at 45° contrasts with previous work[9,14,15] showing faster propagation parallel to muscle fibers. We note here that none of the previous work has been performed on rat muscle, nor

TABLE I. Average speeds of sound±standard deviation (m/s) in freshly excised rat semimembranosus and soleus muscles at 37 °C as a function of muscle fiber orientation to the sound field. $N=10$ for each muscle type. Measurements were taken with either a 6- or 10-MHz center frequency transducer. Standard deviation of the spatially averaged speed within one muscle is typically ~4 m/s, but can be up to ~7 m/s.

Semimembranosus		Soleus	
	speed (m/s)		speed (m/s)
90°	1589±5	90°	1582±3
45°	1581±5	45°	1576±4

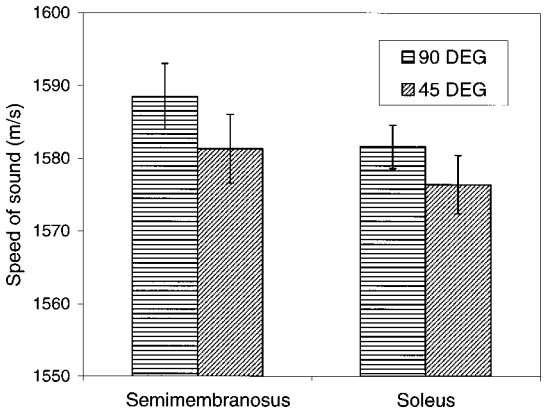

FIG. 9. Speeds of sound averages for the ten semimembranosus and ten soleus muscles measured at 45° and 90°.

apparently on samples that are measured this soon *post-mortem*. For a comparison between our fresh muscle measurements and *post-rigor* rat muscle, two of the same muscle samples for each type were measured one day later (*post-rigor*) after overnight storage in saline in the refrigerator. The speed of sound in each case decreased by close to 1%, indicating some softening, but the propagation speed for the four samples remained faster for the 90° orientation (but the difference was less: 0.2%–0.3% for the *post-rigor* samples).

The backscatter coefficient as a function of frequency is plotted in Fig. 10 for the ten semimembranosus muscles, and in Fig. 11 for the ten soleus. The symbols in each graph represent a different animal, and again the 90° orientation data are joined with solid lines to distinguish them from the values at 45°. In the semimembranosus, the power-law fit (straight line) to the 90° population is clearly a factor of ~30 or more higher than the fit to all the 45° backscatter data, and within each animal, the difference in orientations is at least an order of magnitude. The soleus backscatter data show a similar degree of anisotropy, with fits to the ensemble at each

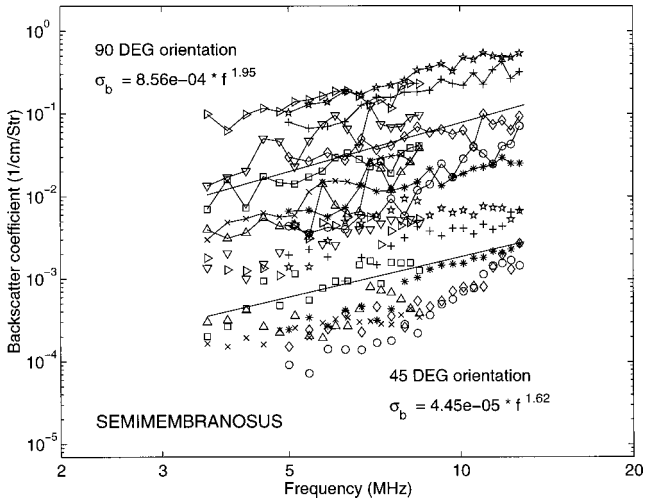

FIG. 10. Backscatter coefficient at 45° and 90° for the ten semimembranosus muscles. Symbols represent individual muscles, and the 90° data have been connected with solid lines to distinguish them from those measured at 45°. Straight lines are power-law fits to all samples at the given orientation. Expressions for each fit are given in the figure (in units of $cm^{-1}\,Str^{-1}$, with f in MHz).

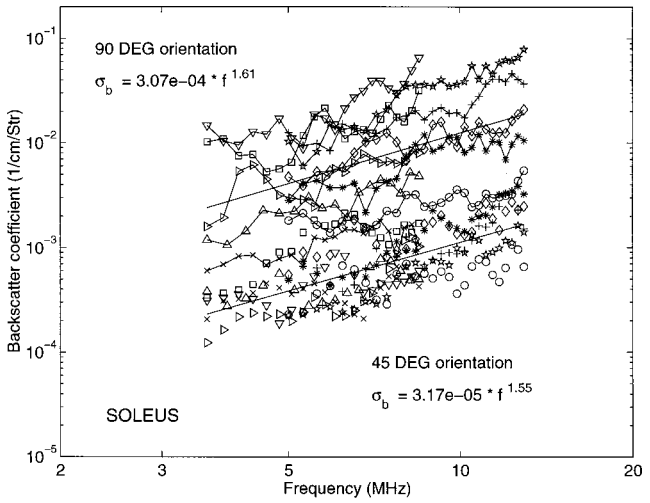

FIG. 11. Backscatter coefficient at 45° and 90° for the ten soleus muscles. Symbols represent individual muscles, and the 90° data have been connected with solid lines to distinguish them from those measured at 45°. Straight lines are power-law fits to all samples at the given orientation. Expressions for each fit are given in the figure (in units of $\mathrm{cm}^{-1}\,\mathrm{Str}^{-1}$, with f in MHz).

orientation a factor 10 apart. Note that $\sigma_b(f)$ values taken by the same method on a homogeneous, isotropic tissue phantom show no difference at all in magnitude or frequency dependence, within experimental uncertainty. The frequency dependence for both muscles and both orientations ranges between $f^{1.5}$ and f^2, with the 90° orientation typically having a slightly higher frequency dependence. A regression analysis of the log–log fits to each muscle and orientation gives $r^2 \approx 0.8$ in each of the four cases ($N=10$).

III. DISCUSSION AND CONCLUSIONS

Distinct differences are observed in the ultrasonic parameters of rat skeletal muscle held with muscle fibers at 90° and 45° to the sound beam. Attenuation values within each muscle show a distinctive increase as the muscle fibers are turned from 90° to 45°, and the ratio of $\alpha_{45°}/\alpha_{90°}$ is consistent at ~2 across the frequency range measured here. This amount of anisotropy is in good agreement with earlier measurements on frozen and *post-rigor* bovine skeletal muscle[9,11–13] and fresh canine myocardium[3] which showed ratios of 1.9 to 3.4 for attenuation parallel versus perpendicular to the muscle fibers ($\alpha_{0°}/\alpha_{90°}$); if one assumes a roughly sinusoidal variation of attenuation with angle of insonification (as seen in the oriented-fiber tissue phantom and canine myocardium samples of Miller *et al.*[3]), this would correspond to $\alpha_{45°}/\alpha_{90°}$ ratios of 1.5 to 2.2.

Speeds of sound in both muscles are seen here to be slightly faster for the 90° orientation, contrary to previous work on fixed and frozen muscle samples,[4,9] and fresh dog,[14] rabbit,[14,15] and frog[15] skeletal muscle. In all cases the difference between speeds measured parallel and perpendicular to the sound beam is on the order of 1% or less, and thus the accuracy of the method for determining sample thickness (which is easier for frozen and fixed tissue) becomes crucial. Although the possibility of systematic error in our determinations of fresh sample thickness exists, a statistical analysis of our propagation speeds at 45° and 90° orientations indicates that our means are distinct. [Note also, an indication of our similar ability to measure speed at both orientations is given by the standard deviation (s.d.) values for the 25 spatial samples of a given muscle and orientation. In comparing s.d.s between orientation groups, the average s.d.s were 3.9 m/s and 4.5 m/s for the 90° and 45° measurements, respectively, with the range in both cases 2–7 m/s.] As a check of our speed of sound technique, a sample of bovine semitendinosis (beef eye of round, grocer preparation) was cut, with sides parallel to muscle fibers, to the approximate size of a rat semimembranosus (0.5 cm thick). Using the same equipment and analysis techniques, including the threshold detection of front and back surfaces to determine sample thickness, the speed of sound was measured with the muscle fibers at 45° and 90° orientations. For this bovine muscle, the speed of sound was measured to be larger at 45° (1553.4 $\pm$3.5 m/s at 21 °C) than at 90° (1547$\pm$3.5 m/s at 21 °C) in agreement with earlier studies on speed of sound in muscle.[4,9,14,15]

The 0.4%–0.5% greater speed in the 90° measurements of rat skeletal muscle seen here may be particular to the rat, in which speed of sound measurements have not previously been measured. The role of freshness was checked with our four *post-rigor* muscle samples, measured in the same manner; although the speeds of sound decreased for the day-old muscles by ~1%, the propagation perpendicular to the muscle fibers remained faster than that at 45°. (The anisotropy did appear to decrease somewhat from ~0.5% to ~0.2% but since only 4 samples were measured compared to the 20 fresh, a quantitative comparison is not valid.) It was not the purpose of this work to examine the *post-mortem* time dependent effects on sound speed, and more measurements will be required to determine under which conditions mammalian skeletal muscle may have faster or slower propagation speeds at a given orientation; but in any case, the anisotropy of speed of sound in fresh tissue is not large.

Backscatter coefficient is the most anisotropic of the measured ultrasound parameters. The average $\sigma_b(f)$ values of the two measured orientations are separated by over an order of magnitude for both the semimembranosus and soleus muscles. The frequency dependence of the backscatter, averaging between $f^{1.5}$ and f^2, is not significantly different between muscles, and although the 90° orientation typically has a slightly higher frequency dependence in a given muscle, the ensemble average for the soleus muscle smears out this difference. (Note that although there is significant variability of the backscatter coefficient values from sample to sample, and the fact that each sample was not measured over the entire frequency range does compromise the frequency dependence, we believe the ensemble of ten samples of each muscle type represents a reasonable statistical sample for showing the magnitude differences and rough frequency dependence of each orientation.)

The frequency dependence of scattering can provide information as to the size of scatterer; Lizzi *et al.*[22] have found a relationship between the frequency dependence of the backscatter (expressed in dB/MHz) and the effective diameter of the scatterers in ocular tissue. Although they assume approximately spherical scatterers, we find it interesting to consider their model in examining our muscle samples of

presumably elongated scatterers. In using their spectral slope relationship, we find from our data an ''effective scatterer diameter'' of approximately 60 μm. Interestingly, a morphometric study of soleus muscle fiber in male and female rats[23] determined a 63–64 μm diameter of the predominantly (90%) type I (slow-twitch) muscle fibers. Our microscope images of both the soleus and semimembranosus muscle (Fig. 1) also indicate muscle fiber diameters on the order of 60 μm. This suggests that the effective scatterers in rat skeletal muscle might be the myofibers, instead of the smaller sarcomeres or myofibrils, or the larger myofiber bundles.

In summary, anisotropy in rat skeletal muscle has been quantified here by characterizing attenuation, speed of sound, and backscatter coefficient as a function of the muscle fiber orientation to the sound field. The anisotropy of speed is seen to be quite small, but attenuation differs by a factor of 2 with 90° and 45° orientation, and backscatter by over an order of magnitude. The mechanisms which produce the anisotropy in these parameters must be related to orientation of the elastic tissue structure, and it seems likely that scatterers of the size of the muscle fibers are involved. More work must be done, however, to uncover the physical causes of the observed ultrasound interaction with biological tissue.

ACKNOWLEDGMENTS

We thank Professor James Zachary, Kandice Spraker, Jim Blue, Professor Phil Best, and Jennifer Mitchell for advice and assistance with the animals, and Professor Timothy Hall for helpful discussions of backscatter data analysis. Special thanks to Professor Zachary for facilitating the microscope images. This work was supported in part by CA09067 from the National Institutes of Health.

[1] J. G. Mottley and J. G. Miller, ''Anisotropy of the ultrasonic backscatter of myocardial tissue: I. Theory and measurement *in vitro*,'' J. Acoust. Soc. Am. **83**, 755–761 (1988).
[2] E. I. Madaras, J. Perez, B. E. Sobel, J. G. Mottley, and J. G. Miller, ''Anisotropy of the ultrasonic backscatter of myocardial tissue: II. Measurements *in vivo*,'' J. Acoust. Soc. Am. **83**, 762–769 (1988).
[3] J. G. Mottley and J. G. Miller, ''Anisotropy of the ultrasonic attenuation in soft tissues: Measurements *in vitro*,'' J. Acoust. Soc. Am. **88**, 1203–1210 (1990).
[4] E. D. Verdonk, S. A. Wickline, and J. G. Miller, ''Anisotropy of ultrasonic velocity and elastic properties in normal human myocardium,'' J. Acoust. Soc. Am. **92**, 3039–3050 (1992).
[5] B. K. Hoffmeister, E. D. Verdonk, S. A. Wickline, and J. G. Miller, ''Effect of collagen on the anisotropy of quasi-longitudinal mode ultrasonic velocity in fibrous soft tissues: A comparison of fixed tendon and fixed myocardium,'' J. Acoust. Soc. Am. **96**, 1957–1964 (1994).
[6] B. K. Hoffmeister, S. M. Handley, E. D. Verdonk, S. A. Wickline, and J. G. Miller, ''Estimation of the elastic stiffness coefficient c_{13} of fixed tendon and fixed myocardium,'' J. Acoust. Soc. Am. **97**, 3171–3176 (1995).
[7] B. K. Hoffmeister, S. E. Gehr, and J. G. Miller, ''Anisotropy of the transverse mode ultrasonic properties of fixed tendon and fixed myocardium,'' J. Acoust. Soc. Am. **99**, 3826–3836 (1996).
[8] C. S. Hall, E. D. Verdonk, S. A. Wickline, J. E. Perez, and J. G. Miller, ''Anisotropy of the apparent frequency dependence of backscatter in formalin fixed human myocardium,'' J. Acoust. Soc. Am. **101**, 563–568 (1997).
[9] W. D. O'Brien, Jr. and J. E. Olerud, ''Ultrasonic Assessment of Tissue Anisotropy,'' 1995 IEEE Ultrasonics Symposium Proceedings, pp. 1145–1148 (1995).
[10] M. F. Insana, T. J. Hall, and J. L. Fishback, ''Identifying acoustic scattering sources in normal renal parenchyma from the anisotropy in acoustic properties,'' Ultrasound Med. Biol. **17**, 613–626 (1991).
[11] V. Roberjot, P. Laugier, and G. Berger, ''Anisotropy in bovine skeletal muscle in vitro: Frequency dependent attenuation and backscatter coefficient over a wide range of frequencies,'' 1994 IEEE Ultrasonics Symposium Proceedings, pp. 1467–1470 (1994).
[12] D. Shore, M. O. Woods, and C. A. Miles, ''Attenuation of ultrasound in *post rigor* bovine skeletal muscle,'' Ultrasonics **24**, 81–87 (1986).
[13] D. K. Nassiri, D. Nicholas, and C. R. Hill, ''Attenuation of ultrasound in skeletal muscle,'' Ultrasonics **17**, 230–232 (1979).
[14] D. E. Goldman and J. R. Richards, ''Measurement of high-frequency sound velocity in mammalian soft tissues,'' J. Acoust. Soc. Am. **26**, 981–983 (1954).
[15] C. R. Mol and P. A. Breddels, ''Ultrasound velocity in muscle,'' J. Acoust. Soc. Am. **71**, 455–461 (1982).
[16] We use a recipe for Tyrode solution from the laboratory of Professor P. Best, Dept. of Physiology, University of Illinois (in mM units): 137 NaCl, 5.4 KCl, 1$MgCl_2$, 0.33 NaH_2PO_4, 10 HEPES (buffer), 2$CaCl_2$; adjust *p*H to 7.4 with NaOH; add dextrose to 290 osmolarity. Original reference: M. V. Tyrode, ''The mode of action of some purgative salts,'' Arch. Internat. Pharm. Thérap **20**, 205–223 (1910).
[17] C.-Y. Wang and K. K. Shung, ''Variation in ultrasonic backscattering from skeletal muscle during passive stretching,'' IEEE Trans. Ultrason. Ferroelectr. Freq. Control **45**, 504–510 (1998).
[18] M. F. Insana and T. J. Hall, ''Parametric ultrasound imaging from backscatter coefficient measurements: image formation and interpretation,'' Ultrason. Imaging **12**, 245–267 (1990).
[19] M. F. Insana, R. F. Wagner, D. G. Brown, and T. J. Hall, ''Describing small-scale structure in random meda using pulse-echo ultrasound,'' J. Acoust. Soc. Am. **87**, 179–192 (1990).
[20] See for example, A. V. Oppenheim and R. W. Schafer, *Digital Signal Processing* (Prentice-Hall, Englewood Cliffs, NJ, 1975).
[21] E. L. Madsen, F. Dong, G. R. Frank, B. S. Garra, K. A. Wear, T. Wilson, J. A. Zagzebski, H. L. Miller, K. Shung, S. H. Wang, E. J. Feleppa, T. Liu, W. D. O'Brien, Jr., K. A. Topp, N. T. Sanghvi, A. V. Zaitsev, T. J. Hall, J. B. Fowlkes, O. D. Kripfgans, and J. G. Miller, ''Interlaboratory comparison of ultrasonic backscatter, attenuation, and speed measurements,'' J. Ultrasound Med. **18**, 615–631 (1999).
[22] F. L. Lizzi, M. Astor, T. Liu, C. Deng, D. J. Coleman, and R. H. Silverman, ''Ultrasonic spectrum analysis for tissue assays and therapy evaluation,'' Int. J. Imaging Syst. Technol. **8**, 3–10 (1997). For an earlier work, see also F. L. Lizzi, M. Ostromogilsky, E. J. Feleppa, M. C. Rorke, and M. M. Yaremko, ''Relationship of Ultrasonic Spectral Parameters to Features of Tissue Microstructure,'' IEEE Trans. Ultrason. Ferroelectr. Freq. Control **34**, 319–329 (1987).
[23] I. Ustunel and R. Demir, ''A Histochemical, morphometric and ultrastructural study of gastrocnemius and soleus muscle fiber type composition in male and female rats,'' Acta Anat. (Basel) **158**, 279–286 (1997).